Theoretical Analysis of the Turbulent Flow of Non-Newtonian Slurries in Pipes

RICHARD W. HANKS and BHARAT H. DADIA

Brigham Young University, Provo, Utah

A theoretical model is derived which permits the analytical calculation of the friction factor-Reynolds number curves for non-Newtonian slurries flowing isothermally in smooth pipes. This model is based upon the Bingham plastic rheological equation of state.

A change of mechanism in the transition phenomenon is observed to occur for $N_{He} = 5\ (10^5)$, where N_{He} is the familiar Hedstrom number. Below this value turbulence is suppressed relative to Newtonian flow, while above this value the transition is delayed but turbulence is enhanced relative to Newtonian flow.

A set of theoretical design curves of friction factor versus Reynolds number covering laminar, transitional, and turbulent flows is calculated and presented for a range of N_{He} values from 10^3 to 10^9.

Considerable effort has been expended in efforts to develop semitheoretical models for the turbulent flow of Newtonian fluids in pipes. Much of this work has centered around the mixing length model of Prandtl, with numerous modifications being proposed by various authors. Although there has been considerable experimental study of the turbulent flow of non-Newtonian slurries in pipes, little progress has been made in developing corresponding analytical models.

Recently Hanks and Pratt (*1*) presented an analysis of the laminar-turbulent transition for pipe flow of non-Newtonian slurries which accurately predicted the critical conditions for all available literature data. Hanks (*2*) presented a theoretical analysis of transitional and turbulent flow of Newtonian fluids in pipes in which he was able to compute the f-N_{Re} curve theoretically from the critical Reynolds number of transition upward.

The purpose of the present work is to combine these two theories to develop a theory of transitional and turbulent flows of non-Newtonian slurries in pipes. This theory will then permit one to compute theoretical design curves of friction factor versus Reynolds number. A significant question raised by Thomas (*3*) will be answered. Thomas observed that deviations of the non-Newtonian slurry friction factor data from the Newtonian curve appeared to be directly related to the non-Newtonian nature of the fluid (*3*). He was unable, however, to show this conclusively, although he suggested that it was.

THEORETICAL ANALYSIS

Because of its mathematical simplicity, the linear Bingham plastic model of non-Newtonian slurry rheology (*4*) will be used here:

$$\tau_{rz} = \tau_0 - \eta \frac{dv_z}{dr} \qquad \tau_{rz} > \tau_0 \tag{1}$$

$$dv_z/dr = 0 \qquad \tau_{rz} \leqq 0 \tag{2}$$

In terms of this model, the laminar flow curve may be expressed as (*1*)

$$q = \frac{\tau_w}{4\eta}\left[1 - \frac{4}{3}\xi_0 + \frac{1}{3}\xi_0^4\right] \tag{3}$$

B. H. Dadia is with S. S. White Company, Staten Island, New York.

The terminus of this laminar flow curve is determined by the relations (*1*)

$$N_{Re_c} = N_{He}\left[1 - \frac{4}{3}\xi_{0c} + \frac{1}{3}\xi^4{}_{0c}\right] \Big/ \xi_{0c} \tag{4}$$

$$\xi_{0c}/(1-\xi_{0c})^3 = N_{He}/16{,}800 \tag{5}$$

To calculate the transitional and turbulent flow field, the total momentum flux will be expressed as (*6*)

$$\overline{\tau}_{rz} = \tau_{rz}{}^{(L)} + \overline{\tau}_{rz}{}^{(T)} \tag{6}$$

where the superscript bars indicate temporal means (*6*), the molecular momentum flux is given by Equations (1) and (2), and the turbulent momentum flux or Reynolds stress $\overline{\tau}_{rz}{}^{(T)}$ is given by a modification (*7*) of Hanks' (*2*) model as

$$\overline{\tau}_{rz}{}^{(T)} = \rho L^2\,(-dv_Z/dr)^2 \tag{7}$$

$$L = k(R_w - r)\,[1 - \exp\,(-\phi\,(R_w - r)/R_w)] \tag{8}$$

In these equations L is a modified mixing length, with k being Prandtl's mixing length constant, and ϕ is a parameter (*2, 7*) which reflects the influence of the critical Reynolds number and the damping of the wall on the turbulent eddies. This parameter may be expressed as (*2, 7*)

$$\phi = \frac{R - R_c}{2\sqrt{2}\,B} \tag{9}$$

R_c can be calculated from Equations (4) and (5) for arbitrary values on N_{He}. It is known (*2*) that $B = 22$ for $N_{He} = 0$.

In terms of the temporal mean momentum flux $\overline{\tau}_{rz}$, the solution (*6*) of the equations of motion for temporally steady, spatially developed turbulent flow is $\overline{\tau}_{rz} = (r/R_w)\overline{\tau}_w$. However, in order to be consistent with the rheological model chosen, it is necessary to add the condition given by Equation (2) to Equation (6). Since $\overline{\tau}_{rz}$ is linear in radial position, we may write

$$\xi_0 = \tau_0/\tau_w = r_0/R_w \tag{10}$$

so that Equation (2) is equivalent to the condition $dv_z/dr = 0$ for $\xi \leqq \xi_0$, if we define a dimensionless position variable $\xi = r/R_w$. Thus, for $\xi < \xi_0$ we may rewrite Equation

(6) in the form

$$0 = \xi_0 - \xi \frac{2\sqrt{2}}{R} \left(-\frac{du^+}{d\xi} \right) + k^2 (1-\xi)^2 (1-E)^2 \left(-\frac{du^+}{d\xi} \right)^2 \quad (11)$$

where

$$E = \exp\left[-\phi (1-\xi) \right] \quad (12)$$

and $u^+ = v_z/\sqrt{\tau_w/\rho}$ is the conventional turbulent dimensionless velocity variable.

By noting that Equation (11) is quadratic in $-du^+/d\xi$, we may solve it directly to obtain

$$-\frac{du^+}{d\xi} = \frac{R}{\sqrt{2}} G(\xi, \xi_0, R) \qquad \xi > \xi_0 \quad (13)$$

with

$$G(\xi, \xi_0, R) = \frac{\xi - \xi_0}{1 + \left\{ 1 + \left(\frac{1}{2} \right) k^2 R^2 (\xi - \xi_0)(1-\xi)^2 (1-E)^2 \right\}^{1/2}} \quad (14)$$

The velocity profile is calculated from Equations (13) and (14) by direct quadrature as

$$u^+ = \frac{R}{\sqrt{2}} \int_\xi^1 G(\xi', \xi_0, R) d\xi', \qquad \xi > \xi_0 \quad (15)$$

$$= \frac{R}{\sqrt{2}} \int_{\xi_0}^1 G(\xi, \xi_0, R) d\xi, \qquad \xi \leq \xi_0 \quad (16)$$

Once the expression for the velocity field is known, the mean velocity $<v_z>$ is readily calculated as

$$<v_z> = \frac{2v^* R}{\sqrt{2}} \left[\frac{1}{2} \xi_0^2 \int_{\xi_0}^1 G(\xi, \xi_0, R) d\xi + \int_{\xi_0}^1 \xi \int_\xi^1 G(\xi', \xi_0, R) d\xi \right] \quad (17)$$

If one integrates the double integral in Equation (17) by parts once and uses Leibnitz' rule, it can readily be shown (7) that

$$<v_z> = \frac{v^* R}{2} \int_{\xi_0}^1 \xi^2 G(\xi, \xi_0, R) d\xi \quad (18)$$

with $v^* = \sqrt{\tau_w/\rho}$. In terms of dimensionless parameters, Equation (18) becomes

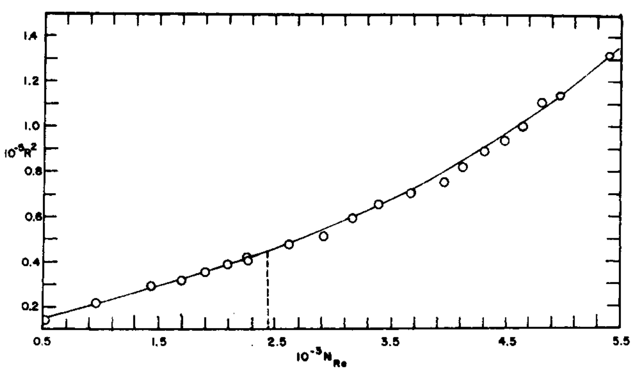

Fig. 1. Comparison of theoretical curves *(solid lines)* with experimental data of Caldwell and Babbitt *(14)* for N_{He} = 1.72 (10^3). For this case, B = 69.2. The vertical dashed line indicates the location of N_{Re_c}.

$$N_{Re} = \frac{1}{2} R^2 \int_{\xi_0}^1 \xi^2 G(\xi, \xi_0, R) d\xi \quad (19)$$

From the definitions of $f = 2\tau_w/\rho <v_z>^2$, N_{Re}, and N_{He}, it is easily shown that

$$R^2 = 2N_{He}/\xi_0 \quad (20)$$

It is now clear that N_{Re} may be calculated from Equation (19) by simple direct gradrature for arbitrarily selected values of $R > R_c$ and arbitrary N_{He}, since for any such pair of values of R, N_{He} the value of ξ_0 is fixed by Equation (20).

RESULTS

Equations (19) and (20) were used to compute curves of R^2 versus N_{Re} for numerous sets of data taken from the literature. The procedure of calculation was as follows. For the given N_{He} of the data, ξ_{0c} and N_{Re_c} were computed from Equations (4) and (5), and then R_c was computed from Equation (20). Then for a series of values of $R > R_c$, Equations (19) and (20) were solved for ξ_0 and N_{Re}, respectively. In this manner, a complete curve of R^2 versus N_{Re} is generated.

In order to make these calculations, one requires numerical values of k and B in Equations (8) and (9). Since the work of Wells (*8*), Ernst (*9, 10*), and Meyer (*11*) indicate no measurable influence of non-Newtonian properties on k, we have assumed the Newtonian value k = 0.36. There is presently no theory available which will permit calculations of B from fluid parameters. Therefore it must be treated as an adjustable parameter. Several values of B were selected and curves of R^2 versus N_{Re} were prepared. The value of B which provided a theoretical curve which appeared to represent best the majority of the data was selected. No statistical curve fitting was performed. Figure 1 is a typical plot for N_{He} = 1.72(10^3) illustrating the results so obtained. Of the numerous sets of data available in the literature, 13 sets from four different investigators which had sufficient turbulent data to permit analysis were used. The results of this analysis are summarized in Figure 2 as a plot of B versus N_{He}. These results may be correlated by the empirical relation

$$B = 157.5 \, N_{He}^{-0.151} \quad (21)$$

for the range $10^3 \leq N_{He} \leq 2(10^9)$.

One might be concerned that the exponent in Equation (21) is inordinately influenced by the single point at N_{He} = 1.6 (10^9) and the group of three points at $N_{He} \simeq 4(10^3)$ since the middle group of points might appear to be represented by a horizontal line. However, this illusion is lost if the single low point at N_{He} = 4(10^3) is ignored. The remainder of the data clearly follows the trend shown.

From Equation (21) we computed values of B for decade values of N_{He} from 10^3 to 10^9 and calculated mean

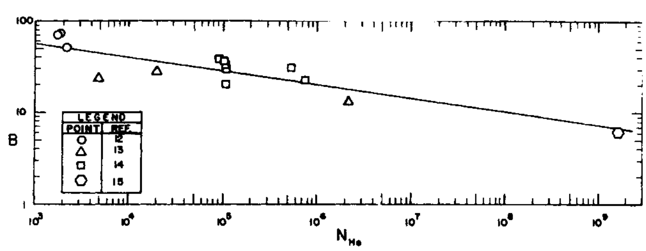

Fig. 2. Correlation of B as a function of N_{He}. The various data points correspond to the data of the authors indicated by the figure legend. The solid line is a plot of Equation (20) and represents the best fit obtained by linear regression.

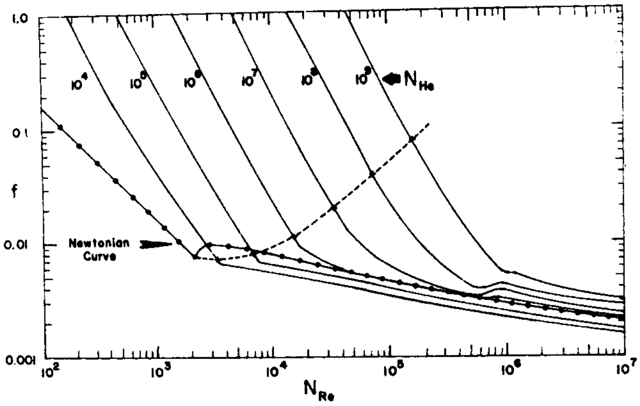

Fig. 3. Theoretical design curves for turbulent pipe flow of Bingham plastic slurries. The Newtonian curve, indicated by the solid circles, is given for comparative reference. The dashed curve passing through the plus symbols is the theoretical locus of critical Reynolds numbers.

design curves of f versus N_{Re}, which are presented in Figure 3. The curve on this plot identified by the solid circles is the ordinary Newtonian ($N_{He} = 0$) curve. These curves represent the average behavior of the data analyzed for this range of N_{He}.

DISCUSSION

That the smoothed curve of B versus N_{He} as given by Equation (21) represents average results is very well illustrated by the data of Thomas (3) for $N_{He} = 4.6 - 4.7$ (10^4) as shown in Figure 4. The solid curve is calculated as described above with $N_{He} = 5\ (10^4)$ and is seen to fall through the average of all the data.

Equation (21) indicates that values of B become increasingly large as N_{He} becomes small. This reflects the purely empirical nature of its origin and emphasizes the danger of extrapolating beyond the limits of the data for which it was determined. Since $B = 23$ for $N_{He} = 0$ (Newtonian fluids), it is clear that for some $N_{He} < 10^3$ the curve must exhibit a maximum. This maximum value could not be determined from the data available in the literature.

Figure 2 also shows a second interesting feature. For $N_{He} < 5(10^5)$ the value of B is greater than the Newtonian value of 23, while for higher values of N_{He} it falls below the Newtonian value. This suggests that for $N_{He} = 5(10^5)$ the turbulent resistance data may fall very close to those for a Newtonian fluid in the same pipe. This is nearly true as is indicated by the curves in Figure 3. However, at higher values of N_{He} a characteristic difference is observed in the f-N_{Re} curves in the development of a maximum in f at high N_{Re} values.

The development of a maximum in the friction factor curve at some Reynolds number in excess of the critical value for $N_{He} > 5(10^5)$ is suggestive of a change in flow mechanism. For N_{He} values lower than this, the f-N_{Re} curves characteristically show a sharp change in slope shortly after N_{Re_c} is reached. Following this abrupt change in slope, the curve closely parallels the standard Newtonian curve for turbulent flow but displaced below it. For higher N_{He} values than $5(10^5)$, this abrupt change is not observed, however. Rather, as N_{Re} increases above the critical value, the friction factor curve drifts gradually away from the laminar curve, goes through a relative minimum, and then rises to a relative maximum. Following this relative maximum, the curve then closely parallels again the standard Newtonian turbulent flow curve. The behavior in this intermediate region is analogous to the transitional flow range ($2{,}000 \leq N_{Re} \leq 4{,}000$) behavior observed for Newtonian fluids except that in the present case it is spread out over a much broader range of Reynolds numbers. Thus the nature of the transition range appears to change as the N_{He} value passes through the vicinity of $5(10^5)$.

The positioning of the turbulent curves in these two kinds of behavior suggests that for $N_{He} < 5(10^5)$ the transition to turbulence is abrupt with the turbulence being suppressed (lower friction losses), while for $N_{He} > 5(10^5)$ the transition to turbulence is suppressed. Once turbulence does ultimately occur, however, it is enhanced (higher friction losses) over the Newtonian case. This interpretation is in keeping with the role of B as a damping parameter for oscillatory motions.

Since the values of B which led to Equation (21) were obtained empirically by curve fitting the experimental data, one might be tempted to discount any interpretations attached to the fact that B differs from 23 as being of no particular consequence. However, one must remember that we are not really just performing empirical curve fitting. Rather, we are selecting values of a parameter which has a definite physical significance so as to do the best job possible of representing the data with the theoretical equation. We note that the form of this equation is rigidly fixed by the theoretical model and we have no assurance that any value of B could be found which would cause this particular model to fit the data at all. The fact that such B values do exist therefore is significant in its own right and lends credence to the model. Therefore deviations of B from 23, particularly when they can be uniquely correlated as a function of the non-Newtonian rheology parameter N_{He}, are significant and cannot be dismissed lightly as fortuitous empirical results. To be sure, a much more detailed and complex analysis is needed before a detailed explanation of why B changes can be given. Such is the fate of all semiempirical theories.

When full turbulence finally is attained, the family of curves falls fairly close together for all N_{He} in accord with Thomas' observation (3). He postulated that all the turbulent data could be correlated by a single curve. Clearly from Figure 3 we can see that this is not true, although for the low Hestrom number range (into which most of his data fell) the scatter of data could well justify such an

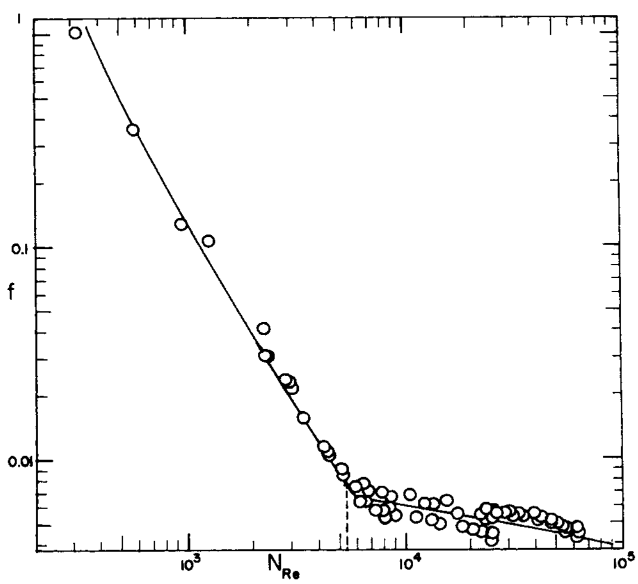

Fig. 4. Comparison of theoretical curves *(solid lines)* calculated with B as given by Equation (20) with the experimental data of Thomas (3) for $N_{He} = 4.7\ (10^4)$. The vertical dashed line indicates the theoretical location of N_{Re_c}.

assumption in the absence of any theory to the contrary. The scatter of his data is evident from Figure 4.

The resistance curves of Figure 3 can be used to design pipe lines for a wide spectrum of non-Newtonian slurries. They represent the industrially important range of non-Newtonian behavior. Further investigation will be required in order to develop a mechanistic explanation for the results of Figure 2 and to verify experimentally the maximum in the high N_{He} curves.

ACKNOWLEDGMENT

This work was supported by National Science Foundation Grant Number GK-1922.

NOTATION

B = damping parameter in turbulent momentum flux model
D = pipe diameter
dp/dz = axial pressure gradient
dv_z/dr = shear rate
E = exponential factor as defined by Equation (12)
f = Fanning friction factor
f_c = critical laminar-turbulent transition value of f
G = shear function as defined by Equation (14)
k = mixing length constant, $k = 0.36$
L = modified mixing length as defined by Equation (8)
N_{He} = Hedstrom number, $D^2\rho\tau_0/\eta^2$
N_{Re} = Reynolds number, $D\langle v_z\rangle\rho/\eta$
N_{Re_c} = critical laminar-turbulent value of N_{Re}
q = $\langle v_z\rangle/R_w$, pseudoshear rate
r = radial position variable
R = $N_{Re}\sqrt{f}$
R_c = $N_{Re_c}\sqrt{f_c}$
R_w = pipe wall radius
u^+ = v_z/v^*
v_z = axial velocity component
$\langle v_z\rangle$ = area mean value of v_z
v^* = $\sqrt{\tau_w/\rho}$

Greek Letters

η = plastic viscosity in Equation (1)
ξ = $r/R_w = \tau_{rz}/\tau_w$
ξ_0 = τ_0/τ_w
ξ_{0c} = τ_0/τ_{wc}
ρ = fluid density
τ_{rz} = axial shear stress or momentum flux
τ_w = value of τ_{rz} at $r = R_w$
τ_{wc} = value of τ_w when $N_{Re} = N_{Rec}$
τ_0 = yield stress in Equation (1)
ϕ = mixing length parameter as defined by Equation (9)

LITERATURE CITED

1. Hanks, R. W., and D. R. Pratt, *Soc. Petrol. Eng. J.*, **7**, 342 (1967).
2. Hanks, R. W., *AIChE J.*, **14**, 691 (1968).
3. Thomas, D. G., *ibid.*, **6**, 631 (1960).
4. Buckingham, E., *Proc. ASTM*, **21**, 1154 (1952).
5. Hedstrom, B. O. A., *Ind. Eng. Chem.*, **44**, 651 (1952).
6. Bird, R. B., W. E. Stewart, and E. N. Lightfoot, "Transport Phenomena," Chap. 5, Wiley, New York (1960).
7. Dadia, B. H., M. S. thesis, Brigham Young Univ., Provo, Utah (1969).
8. Wells, C. S., Jr., *AIAA Preprint No. 64-36* (1964).
9. Ernst, W. D., *LTV Res. Center Rept. No. 0-71000/5R-14* (1965).
10. ———, *AIChE J.*, **12**, 581 (1966).
11. Meyer, W. A., *ibid.*, **12**, 523 (1966).
12. Gregory, W. B., *Mech. Eng.*, **49**, 609 (1927).
13. Wilhelm, R. H., Wroghten, D. M., and W. F. Loeffel, *Ind. Eng. Chem.*, **31**, 622 (1939).
14. Caldwell, H. E., and D. H. Babbitt, *Univ. Ill. Eng. Expt. Sta. Bull. No. 319* (Nov. 1939); *No. 323* (Nov. 1940).
15. Stevens, W. E., Ph.D. thesis, Univ. Utah (1952).

Manuscript received November 11, 1969; revision received March 20, 1970; paper accepted March 24, 1970.

Waves on a Thin Film of Viscous Liquid

JOHN G. B. BYATT-SMITH

University of California, Berkeley, California

In this paper we consider the problem of the flow of a viscous incompressible fluid down an inclined wall. A solution is obtained by assuming that the free surface is a wave of low frequency. The solution is numerical and the results are compared with existing theories and available experimental results.

In this paper we will consider the flow of a viscous liquid in a thin film. Such flows are often observed in everyday life; for example, when rain runs down a window pane or when paint drains from some solid object which has been dipped in it. This is also a subject of importance in chemical engineering and has been studied by experimenters in that field. The character of the flow has been shown to depend largely on the Reynolds number, although surface tension is important in most cases. For example, experiments show that in flow down a vertical